A Fully Integrated 28nm CMOS Dual Source Adaptive Thermoelectric and RF Energy Harvesting Circuit with 110mV Startup Voltage

Yi-Wu Tang, Chien-Heng Wong, Yuan Du, Li Du, Yilei Li, Mau-Chung F. Chang
Electrical and Computer Engineering Department, University of California, Los Angeles, CA 90095

***Abstract*- A fully integrated dual source adaptive thermoelectric and RF energy harvesting circuit is presented. Its boost oscillator, rectifier and boost converter all operate at RF frequency to make inductor and capacitor integration feasible. The oscillator Gm adaptive bias reduces current consumption at higher voltage while assisting startup at lower voltage. The RF input signal further reduces startup voltage through Q-enhanced amplification and super-regenerative mode. Implemented in 28nm CMOS, the self-startup voltage was 110mV without RF input and 85mV at -16dBm input. The boost converter peak output power is 520µW, power conversion efficiency (PCE) is 25% and end-to-end PCE is 10%.**

Keywords—Energy harvesting, self-startup, boost oscillator, boost converter, super-regenerative oscillator

I. Introduction

As wireless sensor networks and internet of things gain traction in industrial, medical and consumer applications, self-powered, energy harvesting circuits become a key enabling technology where direct power is impractical or battery replacement is difficult.

One energy harvesting challenge is the ultra-low available ambient power. A battery-less energy harvesting system thus requires low input DC voltage or RF power for robust startup performance. Because multiple potential energy sources may be available, such as thermoelectric energy from temperature gradients or RF power from various transmitters, multi-source energy harvesters would utilize multiple power sources in combination. Many dual-source harvesters work with different sources that generate the same electrical type, such as thermoelectric, piezoelectric or photovoltaic DC sources [1, 2], or multi-frequency band RF sources [3]. Other dual-source systems combine two harvesting circuits that work independently [4]. A more efficient approach is proposed that allows the dual sources to interact with each other, lowering the startup voltage when both sources are available.

Another challenge is the miniature form factor dictated by certain applications such as implant medical devices, or by cost considerations. A fully integrated solution implies startup options that do not rely on an external battery, mechanical switch [5], large µH~mH transformers/inductors [6, 7], or large nF~µF capacitors [8, 9].

This paper presents a fully integrated energy harvesting system consisting of a boost oscillator startup circuit, an RF rectifier and a boost converter that operate at RF frequency and that completely eliminate off chip components and PCB. To improve energy efficiency, a proposed adaptive bias scheme for the boost oscillator Gm reduces current consumption at higher voltage, while assisting startup at lower voltage.

This paper is organized as follows: Section II describes the energy harvesting system, its building blocks and operation theory. Measurement results are summarized in section III. Section IV concludes with discussion.

II. Theory Of Operation And Circuit Details

A. Dual source thermoelectric and RF energy harvester

Fig. 1 shows the proposed energy harvester block diagram that takes a DC input source and an RF injection signal. It consists of a boost oscillator startup circuit, an RF rectifier, a boost converter and its clock generator. The boost oscillator takes V_{IN} as DC power and RF_{in} as an optional RF input signal to generate oscillation at GHz frequency. Either the oscillator output or the RF input drives the RF rectifier, generating DC output voltages that bias and control the boost oscillator adaptive Gm, boost converter, and converter driver. The boost converter provides output voltage to the load. All four blocks run at RF frequencies, while the bias and control voltages generated by the rectifier are DC signals.

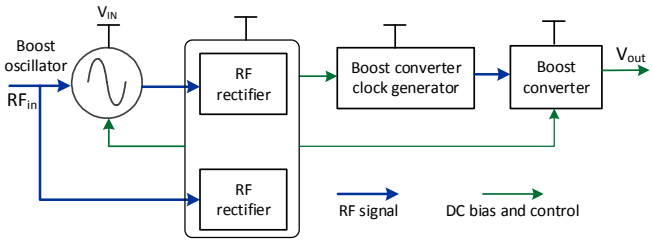

Fig. 1. Block diagram of the proposed dual source thermoelectric and RF energy harvester.

B. Adaptive boost oscillator

As one of the most challenging blocks of an energy harvester, the startup circuitry works at extremely low input voltage (V_{IN}) to enable other harvester circuits that would not function otherwise. Achieving full integration without any off-chip components, the startup circuit is a negative Gm NMOS *LC* boost oscillator shown in Fig. 2. It requires lower headroom and imposes less tank parasitic capacitance than its CMOS counterpart. The startup condition is given by $g_m > 2/R_P$, where g_m is the transconductance of the core devices M1 and M2, and R_P is the oscillator tank equivalent resistance.

To ensure oscillation startup at low input voltage, the circuit needs to generate sufficient g_m and maximize R_P. To obtain sufficient g_m at low supply voltage, a low threshold voltage native NMOS device is used with large *W/L* ratio. To maximize

978-1-5386-2483-8/18/$31.00 ©2018 IEEE

R_P, which is usually dominated by the tank inductor $R_{PL} = Q_L\omega_{osc}L$, an off chip inductor is used in [8] with large inductance L (2μH) and high quality factor Q_L while operating at ~30MHz. However, the oscillation frequency ω_{osc} is an important factor that can boost on-chip tank inductor impedance of merely a few nH and moderate Q_L. If the boost oscillator runs at 1.5GHz, a R_{PL} of 200 Ohm is achievable for a 2nH inductor with a Q_L of 10. Although this is still one order of magnitude smaller than the off-chip inductor case, a comparable low startup voltage is feasible with properly designed Gm.

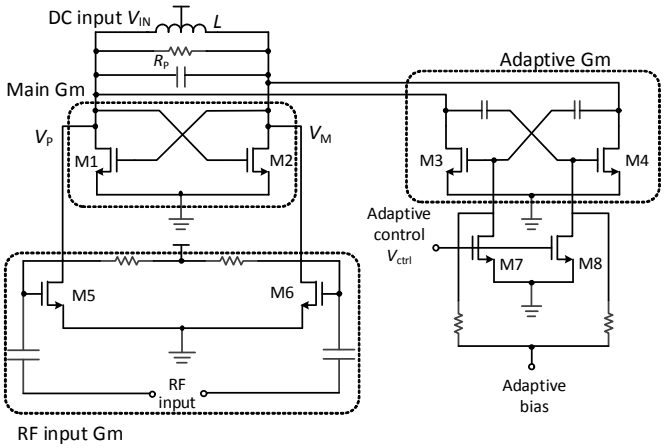

Fig. 2. Adaptive boost oscillator

A small tank impedance mandates large g_m for oscillation startup, leading to large core device size needed at low V_{IN}. At higher V_{IN}, the large core devices consume more current than necessary and reduce power efficiency. A proposed adaptive Gm core solves this problem by partitioning the Gm into the main Gm devices (M1 and M2) and adaptive Gm devices (M3 and M4). The main devices are DC coupled with gates biased at V_{IN}, while the adaptive devices are AC coupled with gate bias controlled by V_{ctrl}, the output of the RF rectifier in the following stage. The rectifier output voltage increases as the oscillation amplitude builds up. When V_{ctrl} is sufficiently high, M7 and M8 will turn on to reduce M3 and M4 gate bias voltages, thus reducing their current consumption. Fig. 3 shows the boost oscillator power saving with adaptive control compared with the case when M3 and M4 are constantly biased at V_{IN}.

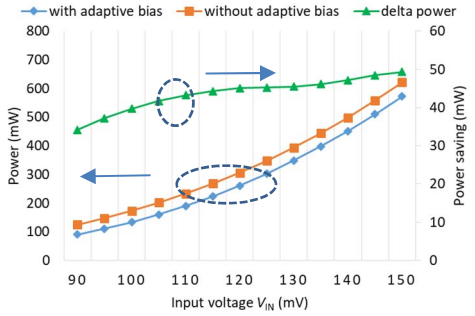

Fig. 3. Boost converter power consumption with and without adaptive bias control

Gm core adjustment has been used in wide tuning range VCO that minimizes tank parasitic capacitance at higher frequency when the tank R_P is larger, and a smaller g_m is needed for oscillation startup and swing [10]. Part of the Gm core size is switched off, depending on the pre-programed frequency, not supply voltage as in the proposed scheme. Without prior knowledge of V_{IN}, the adaptive Gm core in Fig. 2 is configured initially to generate maximum g_m to ensure startup and adaptively reduces power consumption based on the rectifier output, which indicates oscillation amplitude.

C. *Super-regenerative operation*

Super-regeneration has been used in ultra-low power receivers for startup of an oscillator [11]. The oscillation startup time and amplitude depend on the strength of the injected signal. When the DC voltage from thermoelectric energy is not sufficient for reliable startup by itself or requires long startup time, the harvester in super-regenerative mode can utilize the RF input power to enhance the startup condition and reduce the startup voltage.

Applying KCL to the oscillator tank in Fig. 4, we have

$$C\frac{dV}{dt} + \left(\frac{1}{R_P} - G_m\right)V + \frac{1}{L}\int V dt = I_{inj}\sin(\omega t)\,. \qquad (1)$$

The tank voltage V can be solved as

$$V = e^{-\alpha t}e^{j\omega_d t} + \frac{I_{inj}\sin(\omega t+\varphi)}{\sqrt{\left(\frac{1}{R_P}-G_m\right)^2+\left(\omega C-\frac{1}{\omega L}\right)^2}} \qquad (2)$$

where $\alpha = (1/R_P - G_m)/2C$ and $\omega_d = \sqrt{(1/LC) - \alpha^2}$. In Eqn. (2), the first term represents the free running oscillation, while the second is the forced response to the injected signal.

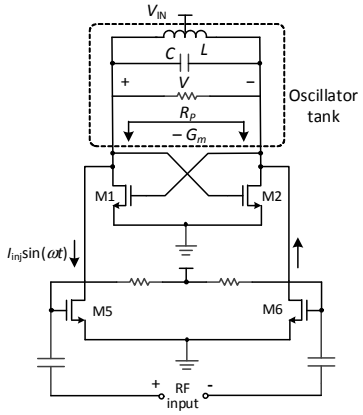

Fig. 4. Super regenerative oscillator with RF injection signal

When G_m is not sufficient at low V_{IN}, and the total tank impedance is positive ($\alpha > 0$), the oscillation cannot start. Negative G_m offsets the tank parasitic resistance R_P and enhances the tank Q. The oscillator operates in the *Q-enhanced amplification mode* for the injection signal and builds up tank swing for harvester startup. When G_m is borderline sufficient to set α negative, the oscillation startup will take a long time. In *super-regenerative mode*, the injection signal provides the initial tank voltage, speeds up startup and enhances oscillation amplitude, as shown in Fig. 5. When G_m is large enough at higher V_{IN}, the oscillator enters *free oscillation mode* and generates sufficient tank swing.

Fig. 6 shows the oscillation amplitude at different input voltage and injection signal amplitude. The injection signal

lowers the threshold V_{IN} voltage for the oscillator to start and increases oscillation amplitude.

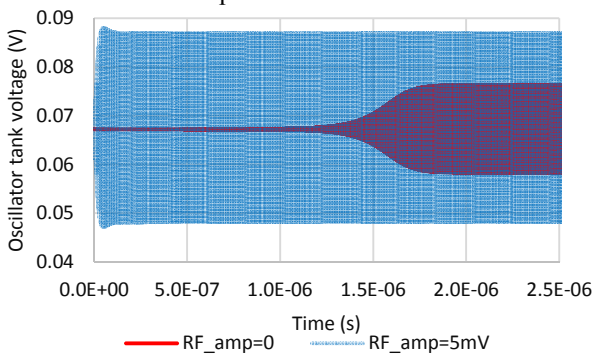

Fig. 5. Boost oscillator startup transient waveforms with and without RF injection signal

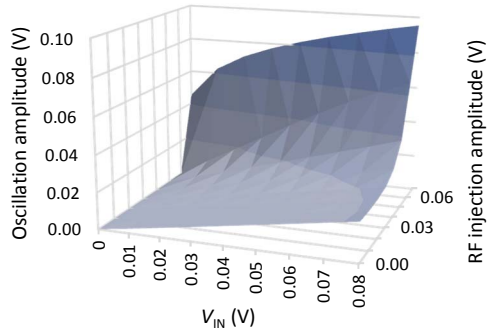

Fig. 6. Oscillation amplitude at different V_{IN} and injection signal strength

D. RF rectifier

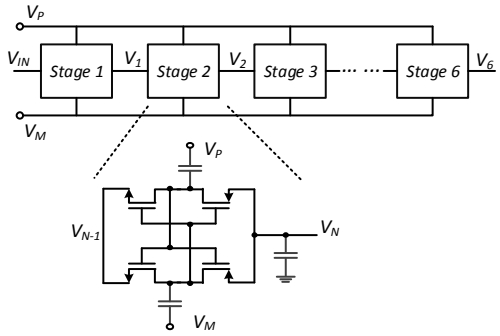

Fig. 7 Multi-stage RF rectifier for DC bias voltage generation

A Pelliconi differential charge pump is used as an RF rectifier [12] to generate DC bias and control voltages driven by RF inputs, which are dual sources from the boost oscillator or the RF injection signal. Shown in Fig. 7, the rectifier consists of 6 stages with differential RF inputs. The output voltage at the N_{th} stage is given by

$$V_N = V_{IN} + 2N\left(V_{amp} - |V_{th}|\right) - I_{out}R_{out} \qquad (3)$$

where V_{amp} is the RF input amplitude, V_{th} is the transistor threshold voltage, I_{out} is the output loading current, and R_{out} is the rectifier output impedance. Large RF swing, low device threshold voltage and small load current are desired for high output voltage. Fig. 8 shows the simulated transient waveform at the output of each stage. The outputs reach the steady state in less than 10µs with a voltage gain from 1.9 at the 1st stage to 6.4 at the 6th stage. The RF rectifier can achieve high voltage gain and high PCE. However, it has limited output power at tens of microwatts and usually drives only large load impedance. We take the rectifier output mainly as DC bias and control voltages with low output current. Therefore high voltage gain can be obtained with I_{out} close to zero in Eqn. (3).

There are two rectifiers implemented, one driven by oscillator tank voltage and the other by the RF injection signal. When V_{IN} is not large enough to start oscillation, sufficient RF input would be able to generate higher DC voltage to bias up the adaptive Gm devices, leading to RF input assisted oscillation at a lower startup voltage.

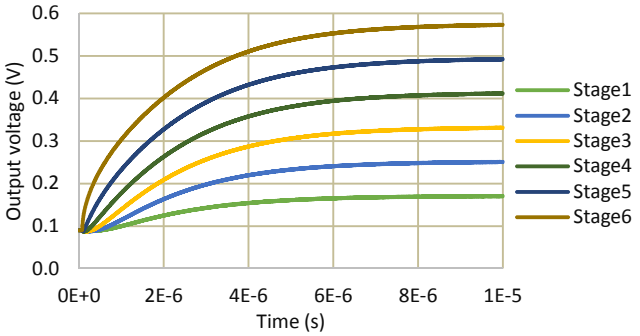

Fig. 8 RF rectifier output voltage of each stage

E. Boost converter

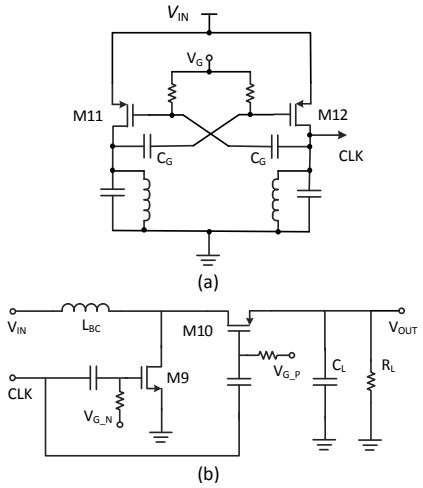

Fig. 9 (a) Boost converter clock generator and (b) boost converter

Boost converters in conventional energy harvesting circuits usually operate at tens of kHz [7] to tens of MHz [8], which require large off-chip capacitance and inductance. Fig. 9 shows the schematics of the proposed boost converter and its clock generator. The output capacitor C_L is determined by the output voltage ripple (ΔV) requirement

$$C_L = \frac{I_{OUT}}{\Delta V \cdot f} \qquad (4)$$

where I_{OUT} is the output current and f is the boost converter clock frequency. For I_{OUT} of 100µA, ΔV of 5mV, a clock frequency of 2GHz will limit C_L to 10pF, which is feasible to be integrated on chip. It is very challenging to generate the clock signal at GHz frequency while meeting the following requirements: 1) large duty cycle (D) to obtain high voltage boost ratio $V_{OUT}/V_{IN} = 1/(1-D)$, and 2) large slew rate to minimize simultaneous turn on time of switches M9 and M10 for high PCE. The boost oscillator output cannot drive the boost

converter as the clock because of its sinusoidal waveform being near 50% duty cycle and low slew rate. A class-C PMOS *LC* oscillator is used with the gates of Gm pair M11 and M12 AC coupled to their drain and biased lower than the drain. Because they are PMOS devices and the class-C operation reduces the turn on time, the drain voltage duty cycle increases and the slew rate is enhanced. By varying the gate bias V_G, the duty cycle and converter boost ratio can be adjusted. Even though the slew rate is ~10GV/s, significantly higher than that of a kHz or MHz clock, the transition phase is not a negligible portion of one sub-nanosecond period, during which the switches M9 and M10 inevitably turn on simultaneously, causing current leakage from V_{OUT} to ground, and resulting in a lower PCE than its lower frequency counterpart.

III. Measurement Results

The dual source energy harvesting circuit was fabricated in 28nm CMOS process. No off chip components were used. It occupies 0.46mm^2 as shown in Fig. 10 including the boost oscillator, the RF rectifier, the boost converter and the converter clock generator. Fig. 11 shows the boost oscillator startup voltage over RF input power. Without RF input, the startup voltage V_{IN} is 110mV with 210µW power consumption. At input power of -16dBm, the startup voltage reduces to 85mV. The boost converter has a peak conversion gain of 2.2, maximum PCE of 25%, and maximum output power of 520µW. Including power consumption of the clock generator and the boost oscillator, the overall peak PCE is 10%. Table 1 shows how the design compares with other designs in the literature. Compared to energy harvesters with off-chip inductors and/or capacitors, the PCE is relatively low due to smaller inductance, lower Q, and higher power consumption at RF frequency. Its startup voltage and maximum output power are comparable with most state-of-the-art designs. Future work would focus on further improvement on inductor Q and boost converter switching efficiency.

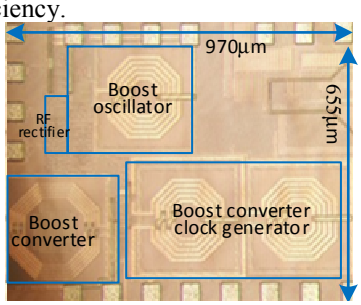

Fig. 10. Die photo

V. Conclusion

This paper presented a fully integrated dual source adaptive thermoelectric and RF energy harvesting circuit. The oscillator Gm adaptive bias reduces current consumption at higher voltage while assisting startup at lower voltage. The RF input signal further reduces startup voltage through Q-enhanced amplification and super-regenerative mode. The boost converter clock is generated by a class-C PMOS *LC* oscillator for higher duty cycle and slew rate. Implemented in 28nm CMOS, it achieved a self-startup voltage of 110mV without RF input and 85mV at -16dBm input. The boost converter PCE is 25% and the overall PCE is 10%.

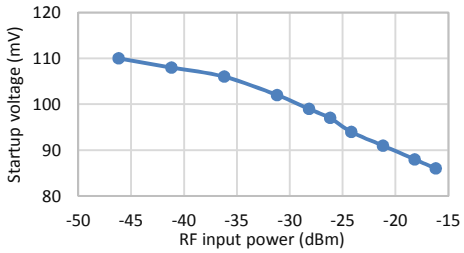

Fig. 11. Measured startup voltage at different RF input power levels

Table I Performance summary and comparison

	JSSC 2013 [8]	JSSC 2015 [9]	JSSC 2014 [6]	JSSC 2016 [7]	This work
Technology	65nm	0.13µm	0.13µm	0.13µm	28nm
Startup mechanism	LC oscillator	Charge pump	XFMR	Charge pump	LC oscillator
Off-chip component	L 2~100µH, C 4.7nF, 1µF	C 10nF x 6	XFMR 10mH	L 200µH C 10^2nH	None
Startup voltage	50mV	150mV	21mV	70mV	110mV w/o RF 85mV w/ RF
Peak efficiency	73%	34%, 72.5%	74%	58%	25% converter 10% end to end
Max. Pout	282µW	608µW	2mW	17µW	520µW

References

[1] S. Bandyopadhyay; A. P. Chandrakasan, "Platform architecture for aolar, thermal, and vibration energy combining with MPPT and single inductor," *IEEE J. of Solid-State Circuits*, pp. 2199-2215, 2012.

[2] A. Shrivastava, *et al*, "A 10 mV-input boost converter with inductor peak current control and zero detection for thermoelectric and solar energy harvesting with 220mV cold-start and -14.5dBm, 915MHz RF kick-start," *IEEE J. of Solid-State Circuits*, pp. 1820-32, 2015.

[3] B. Li, *et al*., "An antenna co-design dual band RF energy harvester," *IEEE Trans. on Circuits and Systems I*, pp. 3256-66, 2013.

[4] Jo Bito, *et al*, "A novel solar and electromagnetic energy harvesting system with a 3-D printed package for energy efficient internet-of-things wireless sensors," *IEEE Trans. on Microwave Theory and Techniques*, pp.1831-42, 2017.

[5] Y.K. Ramadass and A.P. Chandrakasan, "A battery-less thermoelectric energy harvesting interface with 35mV startup voltage," *IEEE J. of Solid-State Circuits*, pp. 333-341, 2011.

[6] Ying-Khai Teh; Philip K. T. Mok, "Design of transformer-based boost converter for high internal resistance energy harvesting sources with 21mV self-startup voltage and 74% power efficiency," *IEEE J. of Solid-State Circuits*, pp. 2694 – 2704, 2014.

[7] J. Goeppert; Y. Manoli, "Fully integrated startup at 70 mV of boost converters for thermoelectric energy harvesting," *IEEE J. of Solid-State Circuits*, pp.1716 – 1726, 2016.

[8] P-S Weng, H-Y Tang, P-C Ku, and L-H Lu, "50mV-input batteryless boost converter for thermal energy harvesting, *IEEE J. of Solid-State Circuits*, pp. 1031-1041, 2013.

[9] J. Kim, *et al*, "A 0.15V input energy harvesting charge pump with dynamic body biasing and adaptive dead-time for Efficiency Improvement," *IEEE J. of Solid-State Circuits*, pp. 414 – 425, 2015.

[10] D. Hauspie, *et al*, "Wideband VCO with simultaneous switching of frequency band, active core and varactor size," *IEEE J. of Solid-State Circuits*, pp. 1472-1480, 2007.

[11] J-Y Chen, M.P. Flynn, J.P. Hayes, A fully integrated auto-calibrated super-regenerative receiver in 0.13-µm CMOS, Journal of Solid-State Circuits, 1976-1985, 2007.

[12] R. Pelliconi, *et al*, "Power efficient charge pump in deep submicron standard CMOS technology," *IEEE Journal of Solid-State Circuits*, pp. 1068-1071, 2003.